Korean J. Chem. Eng., 39(6), 1368-1374 (2022)
DOI: 10.1007/s11814-022-1120-5

pISSN: 0256-1115
eISSN: 1975-7220

RAPID COMMUNICATION

Computational discovery of novel human LMTK3 inhibitors by high throughput virtual screening using NCI database

Anbarasu Krishnan*, Duraisami Dhamodharan, Thanigaivel Sundaram***, Vickram Sundaram***, and Hun-Soo Byun**,†**

*Department of Bioinformatics, Saveetha School of Engineering, SIMATS, Saveetha University, Thandalam, Chennai, Tamil Nadu, India
**Department of Chemical and Biomolecular Engineering, Chonnam National University, Yeosu, Jeonnam 59626, Korea
***Department of Biotechnology, Saveetha School of Engineering, SIMATS, Saveetha University, Thandalam, Chennai, Tamil Nadu, India

(*Received 23 February 2022 • Revised 13 March 2022 • Accepted 20 March 2022*)

Abstract−Breast cancer is the most common cause for women's deaths worldwide. LMTK3 has been demonstrated as critical biomarker for ERα positive breast cancer. It regulates breast cancer by phosphorylating estrogen receptor. Association of LMTK3 in breast cancer is connected with disease free and poor overall survival. In this current computational study, virtual screening was accomplished on human LMTK3 using a large library of NCI database in Schrodinger. From the ligand library, the best compounds were selected and evaluated based on molecular docking using Glide module and their relative molecular dynamics using Desmond. Different parameters like binding energy and interactions like hydrogen bond and hydrophobic contacts have a significant impact on LMTK3 inhibition. Based on docking score, the best lead molecules were separated and analyzed for ADME properties using QikProp tool. Overall, our results confirmed the compounds NCI26194 had been screened from the NCI database, which has the potential to act as key drug molecule for ERα positive breast cancer. In conclusion, our computer aided technique on human LMTK3 has high perspective for the development of novel anticancer agent for breast cancer treatment.

Keywords: LMTK3, Molecular Docking, Molecular Dynamics, ADME

INTRODUCTION

Lemur tyrosine kinase-3 (LMTK3), a type of serine/threonine/tyrosine kinase, has been demonstrated as novel target for ERα positive breast cancer [1]. It acts as a promising biomarker for ERα-positive breast cancer [2]. Breast cancer is one of the most common and serious tumors that affects women today. According to the number of cancer deaths, it is the second most serious malignancy among the different malignancies that can occur [1]. Breast cancer is the leading cause of death in women under the age of 35 and over the age of 75, respectively [2]. Breast cancer is predominantly caused by the female hormone estrogen, which plays a role in the origin and proliferation of cancer cells. LMTK3 plays important role in regulating ERα by phosphorylation and protect ERα from its proteasomal degradation. ERα-positive breast cancers can be treated effectively by blocking LMTK3, which down regulate ERα mRNA expression [3]. Drug screening is required for broader research on classification of specific LMTK3 inhibitors to overcome endocrine resistance and metastasis in breast cancer [4]. Breast cancer is the second most lethal among the various malignant cancers that occurs in women [5]. The most often used treatments for ER-positive breast cancer are anti-estrogens such as tamoxifen, estrogen withdrawal such as aromatase inhibitors, and receptor degradation induction such as fulvestrant, among others [5]. Endocrine resistance in patients with breast cancer is a major stumbling block in the treatment of the disease. In breast cancer, estrogen is the primary female hormone involved in the expansion of cancer cell and progression [6]. Estrogen receptor is a cluster of protein expressed in 70% of breast cancers and is the chief target for breast cancer. ERα positive breast cancer is most common in metastatic stage of breast cancer [7]. Endocrine resistance is the major hurdle in breast cancer treatment [8]. Treatment with the drug tamoxifen, aromatase inhibitors, and drug fulvestrant is the current approach to treating ERα positive breast cancer [9]. Phosphorylation of ERα contributes more to endocrine resistance by controlling its stability and transcriptional activity [10,11]. This family of serine/threonine/tyrosine kinases, known as LMTK3, has been identified as a new target for the treatment of ERα positive breast cancers [10]. This suggests a wide range of tamoxifen resistance mechanisms and is a powerful measure for disease-free survival and overall survival connected to germline polymorphisms predictive and prognostic factor that regulates estrogenic signaling. The ERα-positive breast cancer biomarker has a higher positive selection rate than the chimp ortholog. The kinase inhibitors are considered as effective therapeutics agents for breast cancer as they are found to be target for ERα positive breast cancer [12]. Directing LMTK3 in ERα positive breast cancers is a more effective way of treatment along with down regulation of ERα mRNA expression in cancer cells [13]. Among the

†To whom correspondence should be addressed.
E-mail: hsbyun@jnu.ac.kr

current kinase screening for cancer therapy, human LMTK3 serve as a notable example of a druggable target [14]. In addition to breast cancer target, LMTK3 play as key regulator of oncogenic KIT expression and activity in KIT-mutant GIST and melanoma [15].

Based on sequence and structure homology, protein kinase enzymes are classified into two types of serine/threonine kinases and tyrosine kinases. The arrangements of domain in protein kinase are categorized into eleven conserved sub-domains folded into a larger C-terminal and a small N-terminal lobe. ATP binding is favored by the glycine rich loop (P-loop) in the N-terminal lobe and the phosphorylation activity is regulated by activation loop (T-loop) in the C-terminal lobe [16]. As a result, we are looking for potential inhibitors of human LMTK3 in the NCI database library. Structure-based virtual screening was used using a computational technique to reduce time and expense in the drug creation process [17]. For the purpose of identifying lead candidates, virtual screening based on a three-step methodology with several programs was used. For future drug perception, the pharmacology properties of leads were anticipated using ADME. To optimize the stability and binding affinity of the LMTK3-lead complexes, molecular dynamics simulations were undertaken. Based on the first two eigenvectors, principal component analysis (PCA) was used to interpret protein mobility after ligand binding. Furthermore, advanced binding free energy calculations for lead complexes were done utilizing the MM/PBSA methodology to refine the energy in a dynamic system. Computational and structural analyses revealed the selected lead compounds, which could be used as possible LMTK3 inhibitors.

The novelty of this work is screening a large library through the virtual screening protocol using Schrodinger software with two-phase screening. Many protein targets of cancers have been studied using the virtual screening protocol that acts as novel anti-cancer agents. Protein kinases are the key target for computational virtual screening due to the key role in cancers and also specific nature in the binding affinity with small molecules. The other approaches in the computational studies on inhibitors are ligand-based screening using pharmacophore modeling, QSAR and Machine learning methods. In the present study, screening was performed by NCI database by targeting LMTK3. To enhance the stability of LMTK3-lead complexes molecular dynamics simulations were performed. The properties of leads were estimated by ADME for the future drug perceptive. In this study lead candidates were well characterized using computational approach which can serve as potential LMTK3 inhibitors.

MATERIALS AND METHODS

1. Protein Dataset

Human LMTK3 was used as protein target for the screening from NCI ligands database for the study. The previous reports show that the approved model of LMTK3 protein kinase domain was retrieved from public structure model database (PMDB) identifier no: PM0078692 [16]. LMTK3 protein kinase domain model comprises 279 amino acids with "C"-terminal and "N"-terminal domain. The computational model of human LMTK3 from I-TASSER and recent current experimental structure (PDB code: 6SEQ) was superimposed and showed the structural identity with RMSD 2.87 Å (Supplementary Fig. S1). The major target site of LMTK3 is ATP binding cavity for the inhibition by its key residues reported as Y185 and D284 and the other residues include K177, E181, V263, H264, S265 [16,17].

2. Protein Preparation

In the Schrodinger suite the protein structure of human LMTK3 model was processed with the help of Protein Preparation Wizard [18-20]. It prepares protein by applying biological unit, adding bond order to hydrogen and zero order to metal ions, conversion of selenomethionine to methionine, filling of loop and termini capping [21,22]. The tautomeric and protonation states of Arg, Glu, Asp, His and Lys were changed in accordance with a pH of 7.2. Suitable orientations of Asn and Gln residues were generated. Water molecules above 5.0 Å from the active site were deleted [23]. Then, the protein molecule was subjected to geometry refinement restrained minimization with convergence of heavy atoms to an RMSD of 0.3 Å.

3. Ligand Preparation

For the present study, ligand was obtained from NCI database. Coordinate of each compound was retrieved in the SDF format. 3D format of structural coordinates was energetically minimized using the OPLS -2005 force field at a pH of 7.0 +/− 2.0 [24]. Enumeration of all possible protomers and ionization states for all ligands was done using ionizer at a pH of 7.2. Chiral centers of all the ligand molecules were retained for avoiding stereoisomer generation with a limit of 32 stereoisomers per ligand. Conformers having lowest energy were preferred for all the ligands [25].

4. Molecular Docking

The ligands were docked into the receptor using GLIDE (Grid-based Ligand Docking with Energetics) software. In Schrodinger software, the GLIDE module uses a grid which is based on ligand docking technique, allowing favorable contact between one or more potential ligand molecules and protein receptor [26]. In the Glide module, the default parameter of receptor-grid generation was used to define the active site of the prepared protein. The ligands were docked after the generation of receptor grid [27]. Glide score, which is a measure of receptor ligand complex interaction, was calculated using the equation below:

$$\text{Glide score} = 0.065 \times vdW + 0.130 \times Coul + Lipo + Hbond + Metal + BuryP + RotB + Site$$

where *vdW*=van der Waals energy, *Coul*=Coulomb energy, *Lipo*=lipophilic term in hydrophobic grid potential, *Hbond*=hydrogen-bonding term, *Metal*=metal-binding term, *BuryP*=penalty for buried polar groups, *RotB*=penalty for freezing rotatable bonds, and *Site*=polar interactions in the active site.

5. Molecular Dynamics Simulations

In Schrodinger, molecular dynamics simulation for the LMTK3 Apo and LMTK3-lead compounds was performed with the help of Desmond [28,29]. SPC water model was placed with ligand protein complex. Counterions were added to neutralize the system. SHAKE algorithm was used to restrain the structure of water molecules and hydrogen of heavy bond length [30]. Under the Maestro v9.2, the entire system was simulated. On solute, full system minimization was done for 2000 iteration with onset of 50.0 kcal/mol/Å.2 using Broyden - Fletcher - Goldfarb-Shanno LBFGS) algo-

rithms [31]. NPT ensemble was carried out in molecular dynamics simulation with periodic boundary [32]. The temperature was kept at 300 K and one atmospheric pressure with the help of isotropic scaling and Nose-Hoover temperature coupling [33]. The entire operation was carried out for 25 ns NPT production. The conformation was saved and obtained at intervals of 5 ps. Recording of trajectories was done in every 10 ps. In each trajectory, energy fluctuation and RMSD of the complex was evaluated with respect to time of simulation. Consistency in backbone and RMSF of each residue was checked [34]. The entire molecular dynamics was performed on Intel Xeon(R) CPU @ 2.60 GHz with 16 GB DDR RAM. Schrodinger software was compiled and run under Linux Ubuntu16.04 LTS operating system. All the snaps of docking and molecular dynamics simulation performed under GLIDE were rendered using Schrodinger's maestro interface.

6. ADME Prediction

ADME properties of the compound were obtained from Qikprop ver 3.8 program (QikProp, version 13.8, Schrödinger, LLC, New York, NY, 2013) integrated within Schrodinger [35]. It provides a prediction of the properties that are important physically and pharmaceutically. Since neutralization of the structure was not possible and property generation in the normal mode was affected, ligands were neutralized initially and then subjected to the Qikprop module [36]. After processing the program in the normal mode, there were eight features such as molecular weight, QPlogPo/w, QPlogS, QPPCaco, Rule of five, QPlogHERG, Human Oral Absorption [37].

This was based on Lipinski's rule of five, which assesses the blood brain crossing ability and as well as adequacy of it as drug like molecule. These rules evaluate whether chemical compounds or ligands with certain biological and pharmacological activity have the potential to develop orally active drug in humans. The pharmacokinetics of the drug in the human body with its ADME are an important molecular property that was described by the rule. It has also proved to be reliable in evaluating the drug likeness in compounds [37,38].

RESULTS AND DISCUSSION

1. Molecular Docking

Molecular docking studies were performed to study the detailed molecular interaction between LMTK3 active site and present ligands. Prepared ligands NCI26194 and NCI407941 were docked into the active site of LMTK3. The docking result of the ligands with LMTK3 are given (Table 1). Results of docking simulation for NCI26194 and NCI407941 are 8.358, and −8.251 kcal/mol, respectively, which represent good interaction and high binding affinity with catalytic sites of LMTK3. It was observed in docked complex that NCI26194 was shown to form a direct hydrogen bond with ASP217 and ARG270 along with hydrophobic interactions with MET210, LEU194, LEU218, CYS272, TYR292, LEU273, LEU287, VAL147, ILE139, ALA288, ILE282, LEU274, PHE212, VAL162, TYR285 residue of LMTK3. Finally, when docked complex of NCI407941 and LMTK3 was analyzed, it was shown to form a direct hydrogen bond with ASP217 along with the hydrophobic interaction with CYS272, LEU287, ALA288, ILE139, TYR292, LEU273, VAL147, VAL162, MET210, PHE212, TYR285, of LMTK3 shown in Fig. 1 and Fig. 2.

Table 1. Docking energies and interaction profile of ligands

S. no	Ligand name	Docking score	Glide score	Interaction (H bond)	Other interactions
					Hydrophobic
1	NCI26194	−8.35	−8.38	ASP217, ARG270	MET210, LEU194, LEU218, CYS272, TYR292, LEU273, LEU287, VAL147, ILE139, ALA288, ILE282, LEU274, PHE212, VAL162, TYR285
2	NCI407941	−8.35	−8.38	ASP217, ARG270	VAL162, MET210, TYR285, LEU194, ILE282, LEU218, TYR292, LEU273, ALA288, VAL147, ILE139, LEU287, CYS272, LEU274, PHE212

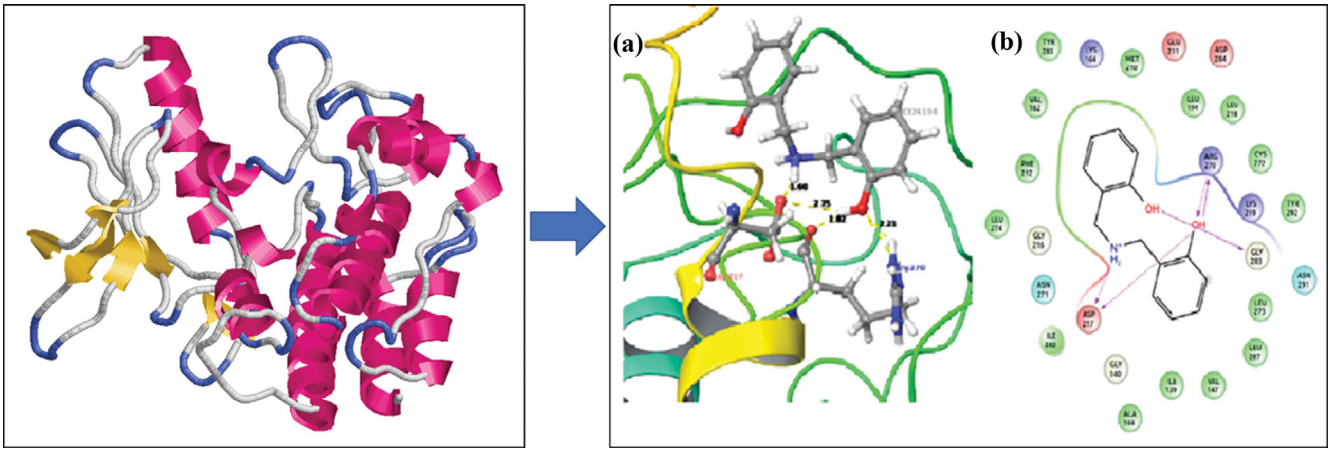

Fig. 1. Docking simulation snapshot of LMTK3 in complex with NCI26194. (a) Showing H-bond and contacts formed by NCI26194 with LMTK3 residues ASP217. (b) 2D snapshot showing various interactions formed by NCI26194 at the catalytically active site of LMTK3.

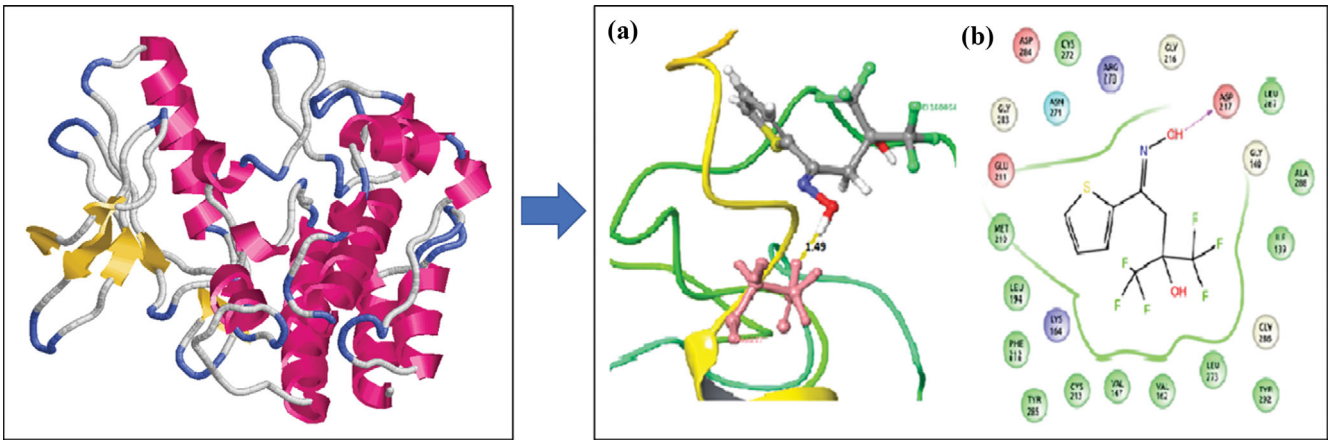

Fig. 2. Docking simulation snapshot of LMTK3 in complex with NCI160054. (a) Showing H-bond and contacts formed by NCI160054 with LMTK3 residues ASP217. (b) 2D snapshot showing various interactions formed by NCI160054 at the catalytically active site of LMTK3.

Table 2. Statistical parameters of MD simulations

Molecule	Statistical parameter									
	Total energy (Kcal/mol)		RMSD (Backbone)		Radius of gyration		Intra molecular H-Bonds		Inter molecular H-Bonds	
	Range	Mean	Range	Mean	Range	Mean	Range	Mean	Range	Mean
LMTK3 (APO)	−8,771.8 to −6,895.2	−7,705.8	0 to 4.1	3.49	19.4 to 20.1	19.8	147 to 208	177.25	NA	NA
NCI26194	−8,505.9 to −6,603.0	−7,482.6	0 to 4.0	3.3	3.0 to 3.7	3.5	165 to 220	195	0 to 4	1.1
NCI407941	−8,995.8 to −7,173.0	−7,931.2	0 to 4.3	3.178	2.6 to 2.9	2.7	148 to 203	180.4	0 to 3	0.9

2. MD Simulations of LMTK3 (apo)

We analyzed the stability of LMTK3 in its native state by plotting the root mean square deviation (RMSD) (Fig. 3(a)) root mean square fluctuations (RMSF) (Fig. 3(b)), radius of gyration (ROG), (Fig. 3(c)) intra-molecular hydrogen bonds (Fig. 3(d)), and energy contributions as the time-dependent function of MD simulations. RMSD of the backbone protein was obtained to be fluctuating around 2.0 Å, with few high peaks up to 3.5 Å in between 2-3 ns of simulated chemical time. Around 6 ns it showed highest fluctuating up to 4 Å. After 5 ns, constant graphs suggested that in each simulated time the protein structure was shown to be stable.

Higher flexibility of the protein region is identified by RMSF of its residue for 25 ns MD simulation. In RMSF graph of LMTK3, we can observe that the major peak of fluctuation has been shown in 160 residues with over 2.8 Å, residue number 210 up to 3.3 Å, residue number 225 up to 3 Å, residue number 300 up to 2.5 Å, residue number 360 up to 2.75 Å. Highest fluctuation in LMTK3 was shown in 325 residues up to 4.25 Å due to presence of loops. We observed that the rest of the residue was stable, and fluctuation was shown below 2.0 Å. ROG of LMTK3 predicts its variation in compactness in the given simulated time. Throughout 25 ns, ROG of LMTK3 in its apo state was observed in the range 19.4-20.1 Å and with an average 19.8 Å. With this data, we can analyze that LMTK3 in its apo state protein is stable without much deviation in overall simulation. Stability of protein structure is dependent upon many factors, such as intramolecular hydrogen bonds present in the protein. LMTK3 in its apo state contains an average of 177 intra hydrogen bonds within a range of 147 and 208 for the 25 ns in molecular simulation. Finally, we observed the total energy for stabilizing the conformation of protein and it was measured in the range of −8,771 and −6,895 kcal/mol with an average of −7,705 kcal/mol. From the above observations we can say that LMTK3 protein structure is stable throughout the 25 ns simulation (Table 2).

3. MD Simulation of LMTK3 in Complex with NCI26194

The effect of ligand NCI26194 binding with LMTK3's catalytic site is observed by performing MD simulation of LMTK3 with NCI26194. Binding energy of −8.35 kcal/mol is obtained from the LMTK3- NCI26194 protein ligand complex from Schrodinger's Glide module. Results of the MD simulation are given in Table 2. RMSF (Fig. 3(a)) for the LMTK3 -NCI26194 complex was calculated, and the highest fluctuation was seen at 160 and 300 residues at 4.2 Å and 4.3 Å, respectively. The rest of the fluctuations were seen below 3.5 Å. RMSD (Fig. 3(b)), for the trajectory of LMTK3 complex with NCI26194 shows fluctuating in the RMSD around 2-2.5 Å in first 5 ns, with few high peaks up to 3 Å between 2-3 ns of simulated chemical time. After that, stabilization of fluctuation was seen and the complex maintained an average of 3.4 Å throughout 25 ns. It was observed that the major active residue of LMTK3 in its apo state was minimized in the presence of NCI26194. We calculated ROG (Fig. 3(c)) of the LMTK3 - NCI26194 complex in the simulated time of 25 ns, which shows steadiness till 9 ns with an average of 3.4-3.5 Å. There is steep fluctuation after 9 ns maintaining an average of 3.6 Å showing instability in protein compactness. Intra hydrogen bonds (Fig. 3(d)) were also analyzed for LMTK3

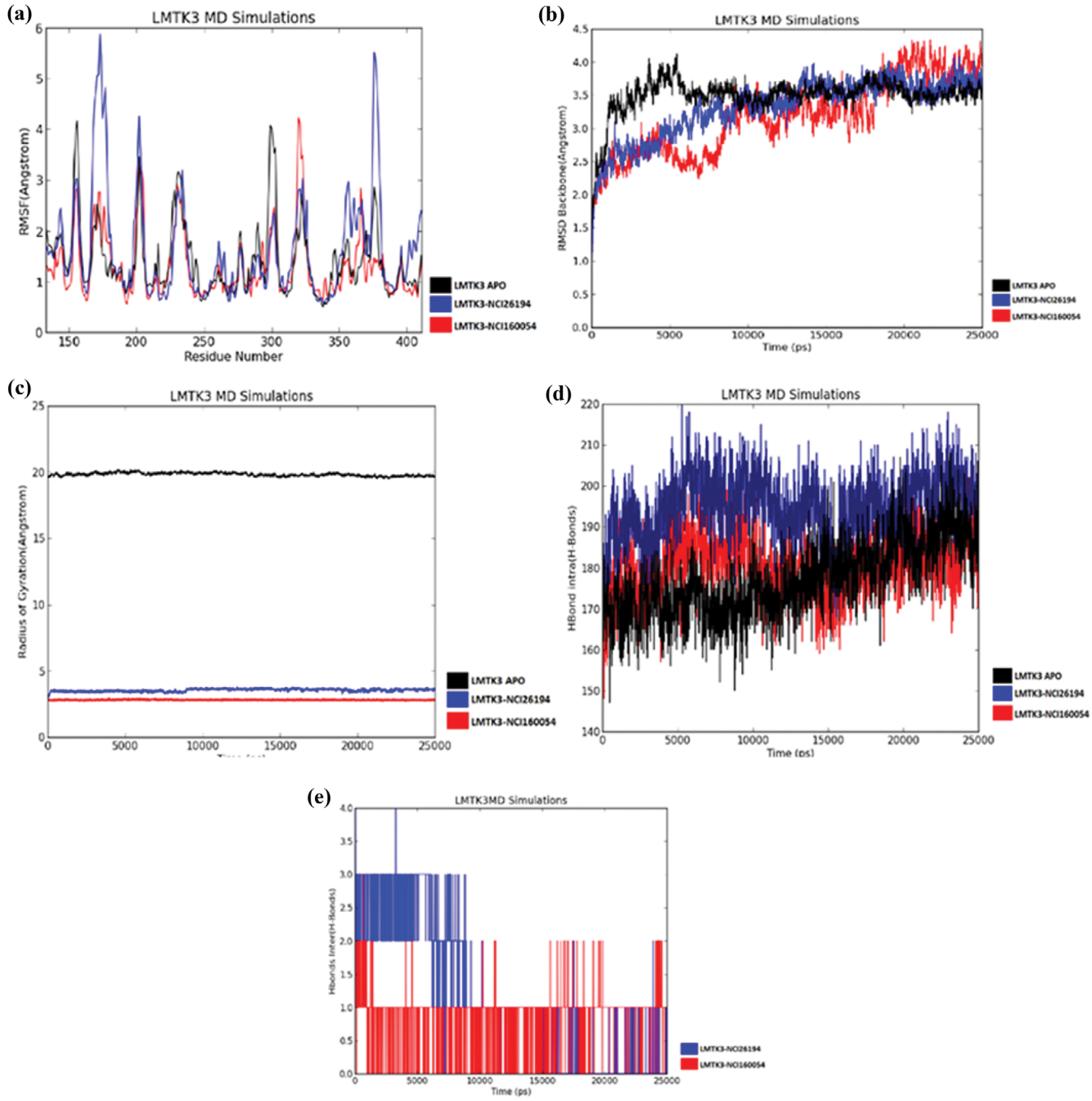

Fig. 3. MD simulation trajectory analysis of LMTK3 protein in presence of no ligand and in complex with NCI26194 and NCI160054 for (a) RMSF (b) RMSD (c) Radius of gyration (d) Total intra molecular hydrogen bonds and (e) Inter hydrogen bonds.

in complex with ligand and found that it is maintaining an average of 195 intra molecular hydrogen in a range 165-220 throughout the 25 ns of simulation time. We also observed an inter hydrogen bond (Fig. 3(e)) of complex, showing an average of 1.18 in a range of 0 and 4. Finally, we analyzed the total energy of LMTK3 - NCI26194 complex involved in the protein stabilization, and it was observed to maintain an average of −7,482 kcal/mol in a range of 8,505 and −6,603 kcal/mol (Table 2).

4. MD Simulation of LMTK3 in Complex with NCI407941

The LMTK3-NCI407941 docked complex was analyzed in MD simulation by a trajectory file obtained from the 25 ns simulation. Using Schrodinger's Glide module, the binding energy of −8.25 kcal/mol was obtained. We calculated RMSF (Fig. 3(a)) for the LMTK3-NCI407941 docked complex, which showed the highest peak at 175 and 360 residues at 5.9 Å and 5.5 Å, respectively, which indicates that protein in this part may have some role in binding to ligand. Initially, the RMSD (Fig. 3(b)) value remained approximately 2.5 Å up to 8 ns, and from 8 to 10 ns the deviations were increased drastically to a maximum of 4.3 Å in the protein. This may be inconsistency of ligand inside the pocket, which could have

Table 3. ADME properties of NCI26194 and NCI407941

Molecule	Mol_MW	QPlogPo/w	QPlogS	QPPCaco	Rule of five	QPlogHERG	Human oral absorption	Percent human oral absorption
NCI26194	229.278	2.011	−1.807	320.093	0	-6.389	3	83.559
NCI407941	307.21	3.012	−2.997	1,778.899	0	-3.41	3	100

resulted in the breakage in hydrogen bond in protein. The ROG (Fig. 3(c)) graph of LMTK3 and NCI407941 complex indicated steep fluctuation at 5 ns at 2.9 Å, which might indicate expansion of protein in that region towards ligand. After that it maintained an average of 2.8 Å throughout the 25 ns of stimulated time. We also analyzed the intra molecular hydrogen (Fig. 3(d)) of complex, which was found to be maintaining an average of 180 in a range of 140 and 208. Inter hydrogen bond (Fig. 3(e)) between LMTK3-NCI407941 complex maintained an average of 0.9 in a range of 0 and 3. Finally, we calculated the total energy of the complex which was involved in stabilizing of the complex and it was found to be an average of −7,931 kcal/mol in a range of −8,995 and −7,173 kcal/mol (Table 2).

5. ADME Properties

We performed ADME studies in QikProp for NCI compounds to obtain pharmacological properties such as molecular weight, MDCK permeability, Caco-2 permeability, QPlogPo/w, QPlogS, QPloghERG, human oral absorption and rule of five to find the drug similarity of the molecules. The molecular weight of NCI26194 and NCI407941 was 229.2 Da and 307.2 Da (Range: 130-725 Da for 95% drug). The Caco-2 permeability for both the NCI compounds was predictable in the appropriate range. The human oral absorption for both the NCI compounds is 3, which shows high absorption. The QPlogPo/w (nm/sec) for NCI26194 and NCI407941 were 2 and 3, respectively (Range: −2.0 − 6.5), whereas the QPlogS for NCI26194 and NCI407941 were −1.8 and −2.9, respectively (Range: −6.5 − 0.5). QPloghERG for the NCI26194 and NCI407941 are −6.3 and −3.4 respectively (Range: Below −5). All these values obtained in these parameters were in the acceptable range, which proves the drug ability of both the NCI compounds (Table 3).

In the current stage of increase in cancer cases and severe side-effects of chemotherapeutic agents reducing clinical efficacy, a successful and specific small molecule is needed that can act as anti-breast cancer agent in order to overcome the endocrine resistance and also the side effects due to chemotherapy. The role of computational screening of a large library will be helpful to identify novel anti-cancer agents that can be future therapeutics for human LMTK3. Further, *in-vitro* and *in-vivo* studies are needed to confirm the inhibition of reported leads from NCI database.

CONCLUSION

A systematic virtual screening approach was followed in the present study to propose NCI compounds as a potent inhibitor of human LMTK3 from small molecules of NCI database. Molecular dynamics for the apo state of LMTK3 showed stability throughout the 25 ns of stimulated time. Molecular docking for best leads was analyzed and the key residues were Asp217 and Arg270. Molecular dynamics simulation was done for the most potent NCI compounds NCI26194 and NCI407941 with LMTK3**.** Among that, NCI26194 interacted well with active site residues such as Asp217 and Arg270 and formed stable H-bond in all trajectories. We compared MD trajectory of native LMTK3 with LMTK3-NCI12694 complex, which showed less variation at structural level and high stability of complex. Finally, molecular dynamic simulations proved that NCI26194 showed better binding orientations, RMSD, RMSF, ROG, inter hydrogen bond and total energy and conformed to good pharmacological properties. Furthermore, we performed hydrogen bond analysis, protein ligand contacts for LMTK3-NCI26194 throughout the 25 ns simulations. Hence, it can be considered for designing lead molecule against LMTK3 and acts as novel anti-breast cancer agent.

ACKNOWLEDGEMENTS

This work was supported by the National Research Foundation of Korea (NRF) grant funded by the Korea government (MSIT) (No. 2021R1A2C2006888). The authors thank Schrodinger for facility and management of Saveetha School of Engineering, SIMATS.

CONFLICT OF INTEREST

The authors declare that there are no conflicts of interest.

SUPPORTING INFORMATION

Additional information as noted in the text. This information is available via the Internet at http://www.springer.com/chemistry/journal/11814.

REFERENCES

1. D. R. Robinson, Y. M. Wu and S. F. Lin, *Oncogene*, **19**, 5548 (2000).
2. G. Giamas, A. Filipovic, J. Jacob, W. Messier, H. Zhang, D. Yang, W. Zhang, B. A. Shifa, A. Photiou, C. Tralau-Stewart and L. Castellano, *Nat. Med.*, **17**, 715 (2011).
3. A. B. Johnson and B. W. O'Malley, *Nat. Med.*, **17**, 660 (2011).
4. Y. Xu, H. Zhang and G. Giamas, *Onco Target*, **5**, 5192 (2014).
5. J. Harris, M. E. Lippman, U. Veronesi and W. Willet, *N Engl. J. Med.*, **327**, 319 (1992).
6. F. Labrie, C. Labrie, A. Bélanger, J. Simard, S. Gauthier, V. Luu-The, Y. Giguere, B. Candas, S. Luo and C. Martel, *J. Steroid Biochem.*, **69**, 51 (1999).
7. J. Stebbing, A. Filipovic and G. Giamas, *Oncotarget*, **2**, 428 (2011).
8. R. C. Wu, J. Qin, P. Yi, J. Wong, S. Y. Tsai, M. J. Tsai and B. W. O'Malley, *Mol. Cell.*, **15**, 937 (2004).
9. S. Ali and R. C. Coombes, *Nat. Rev. Cancer*, **2**, 101 (2002).
10. J. Jiang, N. Sarwar, D. Peston, E. Kulinskaya, S. Shousha, R. C.

Coombes and S. Ali, *Clin. Cancer Res.*, **13**, 5769 (2007).
11. G. Giamas, L. Castellano, Q. Feng, U. Knippschild, J. Jacob, R. S. Thomas, R. C. Commbes, C. L. Smith, L. R. Jiao and J. Stebbing, *Nucleic Acids Res.*, **37**, 3110 (2009).
12. G. Giamas, J. Stebbing, C. E. Vorgias and U. Knippschild, *Pharmacogenomics*, **8**, 1005 (2007).
13. A. B. Johnson and B. W. O'Malley, *Nat. Med.*, **17**, 660 (2011).
14. V. Vella, G. Giamas and A. Ditsiou, *Cancer Gene Ther.*, **24**, 1 (2021).
15. C. Cilibrasi, A. Ditsiou, A. Papakyriakou, G. Mavridis, M. Eravci, J. Stebbing, T. Gagliano and G. Giamas, *Mol. Cancer*, **20**(53), 1 (2021).
16. K. Anbarasu and S. Jayanthi, *Mol. Biosyst.*, **10**, 1139 (2014).
17. K. Anbarasu and S. Jayanthi, *J. Recept. Signal Transduct*, **37**, 51 (2017).
18. A. Lin, Z. Cai, G. Hu and Q. Li, *J. Recept. Signal Transduct*, **35**, 559 (2015).
19. M. Rambabu and S. Jayanthi, *J. Cell. Biochem.*, **120**, 8588 (2019).
20. Schrodinger Suite 2012: Protein Preparation Wizard. Schrodinger, LLC; New York, NY.
21. Schrodinger Suite. Schrodinger, LLC; New York, NY (2012).
22. G. M. Sastry, M. Adzhigirey, T. Day, R. Annabhimoju and W. Sherman, *J. Comput Aided Mol. Des.*, **27**, 221 (2013).
23. K. M. Elokely and R. J. Doerksen, *J. Chem. Inf. Model.*, **53**, 1934 (2013).
24. Schrodinger Suite 2012: LigPrep, version 2.5. Schrodinger, LLC; New York, NY.
25. J. M. Hayes, M. Stein and J. Weiser, *J. Phys. Chem. A*, **108**, 3572 (2004).
26. Glide version 6.1 [software]. New York: Schrödinger LLC (2013).
27. R. A. Friesner, R. B. Murphy, M. P. Repasky, L. L Frye, J. R. Greenwood, T. A. Halgren, P. C. Sanschagrin and D. T. Mainz, *J. Med. Chem.*, **49**, 6177 (2006).
28. Y. Shan, E. T. Kim, M. P. Eastwood, R. O. Dror, M. A. Seeliger and D. E. Shaw, *J. Am. Chem. Soc.*, **133**, 9181 (2011).
29. S. Vilar, J. Karpiak, B. Berk and S. Costanzi, *J. Mol. Graph.*, **29**, 809 (2011).
30. J. P. Ryckaert, G. Ciccotti and H. J. Berendsen, *J. Comput. Phys.*, **23**, 327 (1977).
31. U. Essmann, L. Perera, M. L. Berkowitz, T. Darden, H. Lee and L. G. Pedersen, *J. Chem. Phys.*, **103**, 8577 (1995).
32. W. Shinoda and M. Mikami, *J. Comput. Chem.*, **24**, 920 (2003).
33. S. Nosé, *J. Chem. Phys.*, **81**, 511 (1984).
34. W. Shinoda and M. Mikami, *J. Comput. Chem.*, **24**, 920 (2003).
35. QikProp (Version 3.8). New York, NY: Schrodinger, LLC (2013).
36. C. A. Lipinski, F. Lombardo, B. W. Dominy and P. J. Feeney, *Adv. Drug. Deliv. Rev.*, **23**, 3 (1997).
37. M. Rambabu and S. Jayanthi, *J. Recept Signal Transduct*, **40**, 436 (2020).
38. W. L. Jorgensen and E. M. Duffy, *Adv. Drug. Deliv. Rev.*, **54**, 355 (2002).